Distributed Massive MIMO: A Diversity Combining Method for TDD Reciprocity Calibration

Cheng-Ming Chen[1], Steve Blandino[1,2], Abdo Gaber[3], Claude Desset[2],
André Bourdoux[2], Liesbet Van der Perre[1], and Sofie Pollin[1,2]
[1]Departement of Electrical Engineering, KU Leuven, Belgium
[2]IMEC, Kapeldreef 75, 3001 Leuven, Belgium
[3]National Instruments Dresden, Germany
Email:cchen@esat.kuleuven.be

***Abstract*—Distributed massive multiple-input multiple-output (DM-MIMO) gives a higher spectral efficiency and enhanced coverage area, compared to collocated massive MIMO (CM-MIMO). In general, for massive MIMO, time division duplex is preferable as it enables downlink (DL) precoding based on uplink (UL) channel estimation. A time division duplex (TDD) reciprocity calibration is then essential to compensate the gap between the UL-DL channels, which can be done completely in the base station relying on sounding reference signals (SRS). For a collocated array, relying on mutual coupling between antenna elements, each SRS is received with sufficient power in the array, enabling a reliable estimate of the calibration coefficients. Nevertheless, for DM-MIMO, much less power is collected in distant inter-cluster antennas which degrades the accuracy of the estimated calibration. In this paper, we propose a novel inter-cluster combining method (ICCM) which improves the signal-to-quantization-noise ratio (SQNR) of the SRS, and hence achieves a more robust calibration accuracy for practical DM-MIMO systems. Our experimental results of two 32-antenna arrays distributed in an indoor environment show that ICCM outperforms the existing state-of-the-art algorithms in the sense of lower DL error vector magnitude (EVM) by exploiting diversity and array gain efficiently.**

***Index Terms*—Distributed antenna arrays, large-scale antenna systems, massive MIMO, reciprocity calibration**

I. INTRODUCTION

Massive MIMO (M-MIMO) is an emerging technology which is capable of greatly enhancing the spectral efficiency by serving multiple users at the same time and frequency [1], [2]. To deploy the massive MIMO systems, two paradigms can be considered (see, e.g., [3]–[7]): collocated M-MIMO (CM-MIMO), where the base station (BS) antennas are physically limited to a confined array in the cell center, and distributed M-MIMO (DM-MIMO), where the BS antennas are geographically deployed over the cell and connected with a high speed back-haul. The DM-MIMO system has several advantages compared to the CM-MIMO system such as better decorrelation of channels even for closely collocated users [8], enhanced coverage area and ease of network planning [9], [10]. Nevertheless, in practice, more challenges should be addressed to implement and deploy a DM-MIMO than a CM-MIMO system. Those are the synchronization of distributed local-oscillators, amplifier non-linearities, non-ideal analog filters [11] and the critical time division duplex (TDD) reciprocity. In massive MIMO, the number of BS antennas (hundreds to even thousands) is several orders larger than the number of single antenna mobile stations (MSs). Therefore, for TDD-based massive MIMO, it is more spectrally efficient to obtain downlink (DL) channel state information (CSI) from reciprocal uplink (UL) CSI. Although the physical channel is reciprocal, the baseband-to-RF and the RF-to-baseband conversion chains are generally not [16]. Using the UL CSI is not sufficient to guarantee the effectiveness of user separation in DL, and thus the RF impairments should be compensated.

In this contribution, we concentrate on the practical realization of the TDD reciprocity calibration [13]. Thanks to the idea provided by Argos [15], the reciprocity calibration can be done purely in the BS side and hence no cooperation from MSs is required. For a CM-MIMO system, in which the BS antennas are confined to a limited space, the power of the SRSs used among each of the antenna pairs is also in a limited range, and we can obtain a very good signal-to-noise ratio (SNR) in the SRS during the TDD calibration. Therefore, a full array generalized least square (FA-GLS) method [12], [14], is suitable for solving the TDD calibration problem for a CM-MIMO system. In contrast, for a DM-MIMO system demonstrated in Fig. 1, where the BS antennas are dispersed into several clusters, the FA-GLS method is infeasible for three reasons. First, a larger gain difference between intra-cluster pairs and inter-cluster pairs is observed, which causes a huge burden for fixed-point implementation; second, the huge gain difference, to some extent, leads to non-invertible matrix when solving the FA-GLS problem for DM-MIMO; third, more overheads for sending back the collected SRSs to the center processor are required to calculate the solution. The hierarchical based calibration method presented in [13] provides a good solution to deal with the three aforementioned difficulties for the DM-MIMO system. However, in an arbitrary deployed DM-MIMO system, some anchor nodes were assumed in every cluster for the relative inter-cluster calibration [12], [13], and in reality, the channel between inter-cluster anchor nodes may not be the strongest. In addition to a large distance and path-loss, the channel can be shadowed, suffer from fading or blocked by obstacles as illustrated in Fig. 1.

The main contributions of this paper are summarized in the

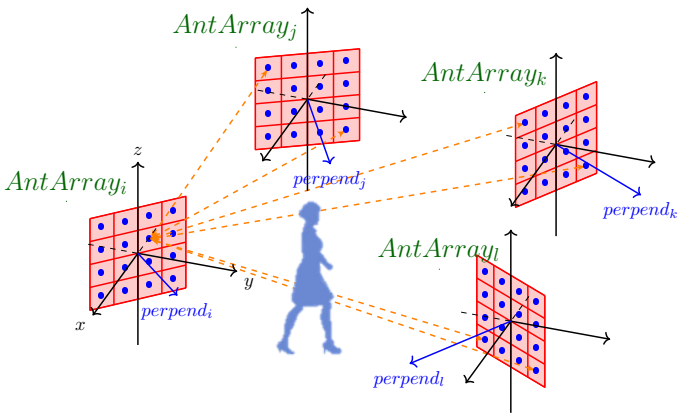

Fig. 1: An illustration of the DM-MIMO system which consists of four distributed clusters of antenna arrays. The Orange arrows stand for sending the SRSs for inter-cluster calibration. Some possible factors degrade the robustness of the inter-cluster reciprocity calibration. For instance, the non-face-to-face in normal lines of the antenna panels or fading in between the arrays degrade the SRSs quality during the inter-cluster calibration. (Note that for a theoretical reason we apply a different configuration than the experiment)

following:

- A hierarchical calibration method has been adopted for DM-MIMO. The novelty is in the proposed inter-cluster combining method (ICCM), where we rely on maximum ratio combining (MRC) and maximum ratio transmission (MRT) to combine multiple SRSs coherently, enabling a power gain and diversity gain.
- The performance of different calibration methods has been compared and evaluated practically using a Massive MIMO testbed with 64 antennas.
- To the best of our knowledge, this is the first work to validate a real DM-MIMO system in DL.

The paper is organized as follows: the system model and the elimination of channel mismatches is described in Section II. Section III presents different calibration methods and the proposed ICCM. The results of the paper are summarized in Section IV, and finally Section V concludes the paper.

The notations in this paper are introduced as the following: Uppercase boldface $\mathbf{A}$ denotes a matrix while lowercase boldface $\mathbf{a}$ indicates a column vector. An $m \times n$ matrix $\mathbf{A}$ can be considered as a side-by-side stack of n column vectors, so we could write $\mathbf{A} = [\mathbf{a}_1\ \mathbf{a}_2\ ...\ \mathbf{a}_n]$. Superscripts T , H and -1 mean the transpose, Hermitian and inverse operation of a matrix, respectively. Moreover, $\mathrm{Tr}(\mathbf{A})$ and $\|\mathbf{A}\|_2$ are the trace and ℓ^2 norm of matrix $\mathbf{A}$, respectively. $\mathrm{abs}(\mathbf{A})$ denotes element-wisely calculation of the absolute value of matrix $\mathbf{A}$. $\mathbf{A} \circ \mathbf{B}$ indicates the Hadamard product of two matrices. Finally, the cardinality of a set B is denoted as $\mathrm{card}(B)$.

II. System Model and the Elimination of Channel Mismatches

A TDD DL massive MIMO with M BS antennas and K single antenna MSs is considered in the system model. With linear precoding, a signal from one subcarrier of the orthogonal frequency division multiplexing (OFDM) modulated symbol is expressed as

$$\mathbf{s} = \sqrt{E_s}\mathbf{W}\mathbf{x}, \tag{1}$$

where $\mathbf{x} \in \mathbb{C}^K$ comprises data symbols from an alphabet χ, and each entry has unit average energy, i.e., $\mathbb{E}\left[\|x_k\|^2\right] = 1$, $k \in \{1, ..., K\}$, so the total transmitted power $E_s = K$. $\mathbf{W} \in \mathbb{C}^{M \times K}$ is the linear precoding matrix, where $\mathbf{W} = \mathbf{V}\mathbf{\Lambda}^{1/2}$, $\mathbf{V} \in \mathbb{C}^{M \times K}$, and $\mathbf{\Lambda} \in \mathbb{R}^{K \times K}$ is a diagonal matrix. The precoding matrix $\mathbf{W}$ satisfies $\mathrm{Tr}(\mathbf{W}^H\mathbf{W}) = 1$ and keeps the precoded vector $\mathbf{s}$ a per-antenna equal power constraint by $\mathbf{\Lambda}$, hence the row $\|\mathbf{w}_k\|^2 = 1/K$, $\forall k$. In TDD reciprocity based massive MIMO, the DL CSI in the BS is estimated from the UL training symbols of the MSs. To differentiate from DL, superscript ul is added for UL only; similarly, to differentiate from RF characteristic in the BS, superscript m is applied for the MS only. The UL channel $\mathbf{H}^{ul} \in \mathbb{C}^{M \times K}$and DL channel $\mathbf{H}$ are not reciprocal because of the transceiver mismatches between the BS and MS. They are expressed as

$$\mathbf{H}^{ul} = \mathbf{R}\mathbf{G}^{ul}\mathbf{T}^m,\ \mathbf{H} = \mathbf{R}^m\mathbf{G}\mathbf{T}, \tag{2}$$

where $\mathbf{G} \in \mathbb{C}^{K \times M}$ stands for the physical channel and $\mathbf{G}^{ul} = \mathbf{G}^T$ within the coherence time; $\mathbf{R} = \mathrm{diag}(r_1, ..., r_M)$ and $\mathbf{T} = \mathrm{diag}(t_1, ..., t_M)$ are the frequency domain RF mismatch factors in the receiver and transmitter, respectively. Due to the RF mismatches, $\mathbf{R}^m$ and $\mathbf{T}$ do not equal to $\mathbf{T}^m$ and $\mathbf{R}$, respectively. Hence, the precoding cannot effectively remove the inter-user-interference (IUI). In [15], it was shown that by right multiplying the transposed UL channel with an inverse of the estimated relative calibration matrix $\mathbf{C} = \gamma\mathbf{T}^{-1}\mathbf{R}$ for some $\gamma \neq 0$, we get a diagonally scaled version of DL channel:

$$(\mathbf{H}^{ul})^T\mathbf{C}^{-1} = 1/\gamma\mathbf{T}^m\mathbf{G}\mathbf{T}. \tag{3}$$

For example, as shown in the zero-forcing precoded signal received at the MSs $\mathbf{y}^m \in \mathbb{C}^K$, the IUI caused by RF mismatches is removed and can be expressed as

$$\mathbf{y}^m = \gamma\sqrt{E_s}\mathbf{R}^m\left(\mathbf{T}^m\right)^{-1}\mathbf{\Lambda}^{1/2}\mathbf{x} + \mathbf{n}^m, \tag{4}$$

where $\mathbf{n}^m$ is the independent identically distributed (i.i.d.) complex Gaussian $\mathcal{CN}(0, N_0)$ noise. The arbitrary complex factor γ and RF channel responses in the MSs can be compensated by the DL channel estimates.

In conclusion, a sufficient accurate estimator for the reciprocity calibration matrix $\mathbf{C}$ is required to cancel out IUI. Fortunately, the calibration can be fully carried out in the BS, and no participation from MSs is required.

III. Estimators of Reciprocity Calibration

The motivation of this paper is to further improve the robustness in the reciprocity calibration of the DM-MIMO system. The proposed ICCM is built on top of the hierarchical based calibration method in [13]. In this section, we introduce first the calibration model between BS to BS antennas and then the FA-GLS algorithm. For DM-MIMO system, the calibration

method is further evolved to the hierarchical based approach. Finally, the proposed hierarchical based ICCM is introduced and some remarks are given to highlight the advantages of ICCM.

A. Sounding Reference Signal

To estimate the diagonal calibration matrix $\mathbf{C}$, SRSs are sent sequentially. Each time, the i_{th} antenna sends a SRS sequence in one OFDM symbol and the other $M-1$ antennas receive. Let $y_{i,j}$ denote the signal received at antenna i when transmitting at antenna j. Signal $y_{i,j}$ and $y_{j,i}$ received in both directions between i and j at each subcarrier are denoted as

$$\begin{aligned} \begin{bmatrix} y_{i,j} \\ y_{j,i} \end{bmatrix} &= \begin{bmatrix} r_i g_{i,j} t_j s_j \\ r_j g_{j,i} t_i s_i \end{bmatrix} + \begin{bmatrix} n_{i,j} \\ n_{j,i} \end{bmatrix} \\ \Rightarrow \begin{bmatrix} c_j & 0 \\ 0 & c_i \end{bmatrix} \begin{bmatrix} y_{i,j} \\ y_{j,i} \end{bmatrix} &= r_i r_j g_{i,j} \begin{bmatrix} s_j \\ s_i \end{bmatrix} + \mathbf{n} \end{aligned}, \tag{5}$$

where the SRS s_i is constrained to have power $\|s_i\|^2 = 1, i \in \{1 \dots M\}$ and can be any predefined sequence in the frequency domain, so for simplicity we assume it equals 1; the physical channels $g_{i,j}$ equals $g_{j,i}$ within the coherence time[1]; $n_{i,j}$ and $n_{j,i}$ are again i.i.d. complex Gaussian $\mathcal{CN}(0, N_0)$ noise. To improve the signal quality of received SRSs, the reference antenna is usually the center antenna. Without loss of generality, we assume antenna 1 as the reference and set the calibration factor c_1 as a common factor γ. By isolating a complex multiplicative γ from the calibration matrix $\mathbf{C}$ and stacking it in a vector format, we get $\mathbf{c} = [1, c_2, ..., c_M]^T$.

B. Full Array Generalized Least Squares (FA-GLS) Algorithm

When the antennas are collocated in a confined array, the line-of-sight (LoS) mutual coupling are quite similar which leads to similar signal to quantization noise ratio (SQNR) between any pair of neighboring antennas. Therefore, the calibration coefficients can be estimated jointly by a FA-GLS algorithm, and a joint cost function is formulated as [13]

$$J_{cal}(\mathbf{c}) = \sum_{i,j \neq i} \left| c_i y_{j,i} - c_j y_{i,j} \right|^2. \tag{6}$$

After constraining c_1 to 1, the LS closed-form solution is represented as

$$\hat{\mathbf{c}} = [1 \quad -(\mathbf{A}_1^H \mathbf{A}_1)^{-1} \mathbf{A}_1^H \mathbf{a}_1]^T, \tag{7}$$

where $\mathbf{A} = [\mathbf{a}_1 \, \mathbf{A}_1]$, $\mathbf{A}_1$ is the rest $M-1$ columns and $\mathbf{A}$ is formulated as

$$\mathbf{A}_{i,j} = \begin{cases} \sum_{n=1, n \neq j}^{M} |y_{n,j}|^2, & i = j \\ -y_{i,j}^* y_{j,i}, & i \neq j \end{cases}. \tag{8}$$

[1]The duration of all M SRSs transmission should be limited to the coherence time

C. Traditional Hierarchical (TH) Calibration Method

For distributed BS antennas, as the arrays are dispersed over a wide area, path-loss between inter-clusters is generally much larger than that within a cluster[2]. Therefore, an alternative approach called traditional hierarchical (TH) calibration method [13] was proposed. Suppose that there are O clusters with an equal number of S antennas in each cluster, i.e., $M = O \cdot S$. The idea behind TH is that for each distributed array, we apply the previous method from (7) to obtain intra-cluster calibration coefficients. Afterwards, a relative calibration concept comes in to calibrate the clusters with respect to each other.

To introduce the inter-cluster calibration method, let (i, o) be the i_{th} antenna in the o_{th} cluster. Suppose that we have obtained the intra-cluster calibration factor $(\hat{c}_i)_o$, the exact calibration coefficient $c_{(i,o)}$ can then be approximated as

$$c_{(i,o)} \approx (\hat{c}_i)_o . c_o, \tag{9}$$

where c_o stands for the inter-cluster calibration coefficient. To determine the inter-cluster calibration coefficient c_o, we first reformulate the received SRS between clusters as $\tilde{y}_{(i,o),(j,p)}$ to replace (5), with the SRS be pre-multiplied by the intra-cluster calibration coefficient $(\hat{c}_i)_o$,

$$\tilde{y}_{(j,p)(i,o)} = r_{(j,p)} t_{(i,o)} g_{(j,p)(i,o)} (\hat{c}_i)_o + n. \tag{10}$$

Particularly noteworthy, as the dynamic range of path-loss between intra-cluster and inter-cluster is significantly large in DM-MIMO, a second time of receive gain adjustment before the start of inter-cluster calibration is beneficial in improving the SQNR. We then define a set of $\varpi_{i,j}$ paths[3] in responsible for sending inter-cluster SRSs between cluster o and p. Finally, a joint inter-cluster cost function can be derived as

$$J_{int} = \sum_{o,p \neq o} \sum_{\varpi_{i,j}} \left| c_o \tilde{y}_{(j,p),(i,o)} - c_p \tilde{y}_{(i,o),(j,p)} \right|^2, \tag{11}$$

The corresponding $\mathbf{A}$ matrix to solve the inter-cluster LS problem is given by

$$\mathbf{A}_{o,p} = \begin{cases} \sum_{q=1, q \neq o}^{O} \sum_{\varpi_{i,j}} \left| \tilde{y}_{(i,q),(j,p)} \right|^2, & o = p \\ \sum_{\varpi_{i,j}} -y_{(i,o),(j,p)}^* y_{(j,p),(i,o)}, & o \neq p \end{cases}. \tag{12}$$

The inter-cluster calibration can be visualized in Fig. 2, where nine antennas in each of the two clusters are presented. Here, two candidate antennas are chosen in each cluster to form a total of four connections. Assigning more antennas in a cluster increases SNR as formulated in (12) but it also decreases the system efficiency.

D. Hierarchical based Inter-Cluster Combining Method (ICCM)

In order to increase the quality of estimation in between the distributed arrays, more candidate antennas have to be considered in the inter-cluster calibration. However, more SRSs transmission also means more overhead. In addition, we

[2]Here we focus on several collocated sub-arrays in a DM-MIMO

[3]If an equal number $S_{cl} \leq S$ of antennas is selected in each cluster, the number of paths is $\mathrm{card}(\varpi_{i,j}) = S_{cl}^2$ between any two clusters.

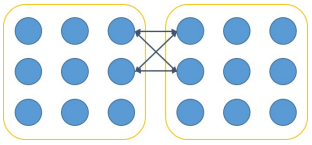

Fig. 2: The inter-cluster calibration of TH method: Four connections are formed for inter-cluster calibration if $S_{cl} = 2$ in one cluster.

should keep in mind that the coherence time of inter-cluster channels should be much shorter than that of LoS channels within a cluster. Furthermore, there is no deterministic way of choosing candidate antennas as channels between inter-cluster subject to shadowing and fading.

The question is how to minimize the time overhead for sending SRSs while maximizing the signal quality. A novel finding behind the proposed ICCM is that after intra-cluster calibration compensation, all elements in a cluster can represent their cluster jointly and hence transmit or receive the SRS coherently to boost array and diversity gain.

We introduce ICCM by defining two kinds of clusters, i.e., master and slave clusters. First, a master cluster broadcasts SRS from a single reference antenna to all antennas in slave clusters. Next, each slave cluster sequentially transmits one SRS by MRT with all antennas in that cluster back to the master cluster. The key point is that MRT is a closed-loop MIMO technique, so the SRS transmitted by MRT can only be coherently combined in the corresponding master cluster. Until now, we build only the connection between one master and the other slave clusters.

By assigning master clusters in an iterative way, the estimation accuracy is further improved by establishing the connections among all clusters. If we have O clusters of arrays in the distributed system, a total of $O-1$ iterations are then required to make a complete interconnection. In the o_{th} iteration, $o \in \{1, ...O\}$, the o_{th} cluster is set as the master cluster, and the rest $O-o$ clusters with indices from $(o+1)_{th}$ to O_{th} are assigned as the slave clusters. An example of four antenna arrays sending the SRS in four steps in the first iteration is demonstrated in Fig. 3. There are five antennas in each array; red grid represents the transmit antenna and blue downward-diagonal denotes as the receive antenna. Starting from the upper-left corner, one SRS is transmitted from the reference antenna in the master cluster to all antennas in the other slave clusters. Meanwhile, all antennas in each slave cluster receive the SRS from the master cluster and combine the signal by MRC. Then, in step two to four, the slave clusters sequentially transmit SRSs back to the reference antenna in the master cluster by MRT. With these four slots of SRSs transmission, the master cluster builds connections with the other three slave clusters. When all the inter-connections are completed, we get a cost function of the ICCM based inter-cluster calibration:

$$J_{\texttt{ICCM}} = \sum_{o,p\neq o} \sum_{\varpi_i} \left| c_o \beta_{p,(i,o)} - c_p \alpha_{(i,o),p} \right|^2, \qquad (13)$$

where ϖ_i is a set of candidate antennas in the master cluster. To save bandwidth and for simplicity, in this paper, it is set to be a single reference antenna, same as the one in the intra-cluster calibration. (we keep the summation in the function to be more general) Moreover, the MRC combined signal,

$$\beta_{p,(i,o)} = \sum_{j=1}^{S} d_{(j,p),(i,o)} \tilde{y}_{(j,p),(i,o)} = \mathbf{d}_{p,(i,o)}^T \tilde{\mathbf{y}}_{p,(i,o)}; \qquad (14)$$

and the MRT signal $\alpha_{(i,o),p}$ is derived as

$$\alpha_{(i,o),p} = \hat{r}_{(i,o)} (\mathbf{g}_{(i,o),p} \circ \hat{\mathbf{t}}_p)^T \mathbf{d}_{p,(i,o)} + n. \qquad (15)$$

where $\hat{\mathbf{t}}_p = [\hat{t}_{(1,p)} ... \hat{t}_{(S,p)}]^T$ and $\hat{r}_{(i,o)}$ stand for the equivalent transmit RF and receive RF impairments after intra-cluster compensation, respectively. The MRT and MRC share the same combining coefficients, $\mathbf{d}_{p,(i,o)}$. Nevertheless, if we apply traditional MRC, we will end up in losing the inter-cluster calibration coefficients. Explained briefly, we review again the receive SRS in the master cluster:

$$\tilde{y}_{(j,p)(i,o)} = \hat{r}_{(j,p)} \hat{t}_{(i,o)} g_{(j,p)(i,o)} + n. \qquad (16)$$

When $\tilde{y}_{(j,p)(i,o)}$ is multiplied by its complex conjugate as the traditional MRC does, phase of RF-impairment term $\hat{r}_{(j,p)} \hat{t}_{(i,o)}$ is also canceled out. To solve this, we design a simple method of calculating the MRC coefficients in three steps:

- Find the index ζ of the maximum path in $\tilde{\mathbf{y}}_{p,(i,o)}$, $\zeta = \underset{j}{\text{argmax}} |\tilde{\mathbf{y}}_{p,(i,o)}|$, where j is the antenna index in the slave cluster p. We choose the maximum path to improve SNR and the accuracy of the estimate.
- Align the phase of all S paths to the strongest path ζ. We get the phase of the MRC coefficients $\angle \mathbf{d}_{p,(i,o)} = \angle \tilde{y}_{(\zeta,p),(i,o)} \mathbf{1} - \angle \tilde{\mathbf{y}}_{p,(i,o)}$, where $\mathbf{1}$ is an $S \times 1$ all-one vector.
- Normalize the amplitude of MRC coefficients for a fair comparison to TH method when applying MRT from a slave cluster[4]. The normalized amplitude of the MRC coefficients are $\text{abs}(\mathbf{d}_{p,(i,o)}) = \text{abs}(\tilde{\mathbf{y}}_{p,(i,o)}) / \left\| \tilde{\mathbf{y}}_{p,(i,o)} \right\|_2$.

Finally, we obtain the corresponding $\mathbf{A}$ matrix:

$$\mathbf{A}_{o,p} = \begin{cases} \sum_{q \not\gtrless o}^{O} \sum_{\varpi_i} \left| \beta_{q,(i,o)} \right|^2 + \\ \sum_{q \not\lessgtr o}^{O} \sum_{\varpi_i} \left| \alpha_{(i,o),q} \right|^2, \ o = p \\ \sum_{\varpi_i} -\alpha^*_{(i,o),p} \beta_{p,(i,o)}, \ o < p \\ \sum_{\varpi_i} -\beta^*_{o,(i,p)} \alpha_{(i,p),o}, \ o > p \end{cases}. \qquad (17)$$

Some remarks are given here:

- Compare (12) and (17), ICCM combines the SRS in the very inner loop of the summation. Suppose there is a big dynamic range in the channel gain, ICCM is more robust in the quantization error. This can be observed from (15), the SRSs are combined over-the-air before the RF front-end.
- Under the same condition that both $\text{card}(\varpi_{i,j})$ and $\text{card}(\varpi_i)$ equal to 1 in TH and ICCM, respectively. Each received SRS in ICCM is a combining of S paths, which benefits from both array and diversity gain.

[4]In a practical implementation, this is not essential. However, we applied this in our experiment section for a fair comparison to the TH method.

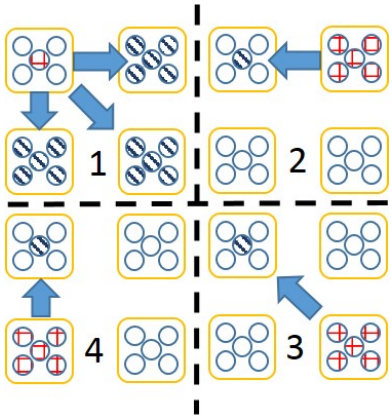

Fig. 3: First iteration in the inter-cluster calibration of ICCM algorithm: Five antennas in each of the four clusters are demonstrated in this example. Red grid antennas transmit, blue downward-diagonal antennas receive and unfilled antennas keep idle. In the first sub-figure, the upper-left cluster plays as the master cluster, and only one reference antenna in the cluster transmits SRS. Meanwhile, the other three slave clusters receive SRS simultaneously. Each slave cluster combines the received SRS by MRC. Then, each slave cluster applies MRT in the SRS to the master cluster sequentially in steps two to four.

IV. Evaluation of Calibration Methods in the Massive MIMO Testbed

In order to exhibit the robustness of ICCM for DM-MIMO systems, we validate the performance of the three algorithms, i.e., FA-GLS, TH and ICCM in the University of Leuven (KUL) massive MIMO testbed. A simulation based evaluation is not considered here, as there is no existing path-loss and mutual coupling models which consider both the inter-cluster and intra-cluster arrays. We target for a real distributed case, as we want to validate a big impact from the fixed-point quantization when there is a larger inter-cluster path-loss compared to the intra-cluster mutual coupling. The effect of big difference in channel gain enables us to show the advantages of ICCM over the other two methods.

A. Description of the Scenario

The experiment was conducted in the lab as shown in Fig. 4. The KUL massive MIMO testbed is a 64 antennas version of Lund's [17]. The testbed were distributed into two subsystems and each of them were connected to a 32-element patch antenna array. The antennas were co-polarized and arranged in the array with one-half wavelength spacing and were operated in 20 MHz bandwidth at 2.6 GHz. The two antenna panels were perpendicular to each other and were separated by a distance of around 2 m. To enlarge the path-loss in between clusters, LoS paths were blocked by absorbers[5]. To synchronize both subsystems, a common source is used to provide the sample clock and time alignment. Moreover, two MSs were placed in between and separated by around 30 cm. Even with only two MSs, if the channel is non-reciprocal, user separation would still be a challenge as we will see in the results.

[5]We could not separate the two subsystems even further to enlarge path-loss due to a hardware limitation, a PXIe connection is required to connect the two.

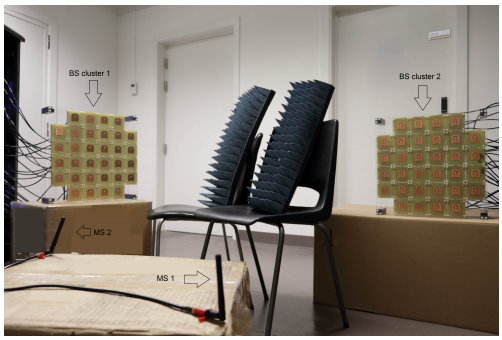

Fig. 4: A two 32-antenna DM-MIMO BS station in the lab. To enlarge the path-loss by blocking LoS in between the clusters, two absorbers were placed in between the arrays. By the time the reciprocity calibration is done, the uncoded 64-QAM DL data will immediately be sent to the two MSs.

B. Intra-cluster Mutual Coupling and Inter-cluster Path-loss Measurement

Measurement was conducted with KUL testbed to validate the power difference between the mutual coupling within an array and the path-loss between the two arrays. Fig. 5 shows the measured mutual coupling with different antenna spacings in an anechoic chamber and the lab. When the antennas are close to each other, with one antenna spacing, we got quite similar results for the two environments. As antenna spacing increases, a slightly higher power contributed from multipaths was observed in the lab. A higher variance in the collected power was also observed when the antenna spacing increased in both scenarios. Consequence, it can be concluded that within a cluster there is always a pair of neighboring antennas which share a very strong and similar level of mutual coupling.

We demonstrate the path-loss between the two clusters for all bi-directional $32 \times 32 \times 2$ paths in Fig. 6. The measurement exhibits a big variance of about 17dB, which validates that the MRC and MRT are indeed beneficial in collecting the diversity gain. If we compare the peak power of mutual coupling (-23dB) to the mean of the path-loss (-48dB), we get equivalently a difference of 4 bits in fixed-point precision. For hierarchical based approach, the impact should be smaller, as the automatic gain control (AGC) can be set separately for both intra and inter-cluster calibrations.

C. Error Vector Magnitude (EVM) and Throughput Evaluation

As the RF-to-RF impairment is an unknown, we directly validate the accuracy of reciprocity calibration by measuring the EVM of the DL uncoded 64-QAM and the achieved throughput. They were recorded simultaneously just after finishing the reciprocity calibration. A moving average with a window size of 25 seconds was applied to smooth out the collected data. During the calibration, the reference antennas were assigned to the center of both arrays. $\mathrm{card}(\varpi_{i,j})$ and

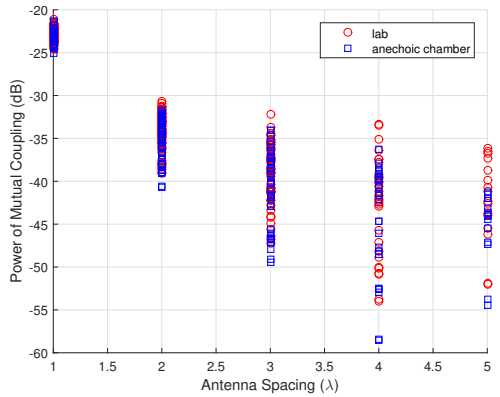

Fig. 5: Intra-cluster mutual coupling measured at the 32 antenna array in both the lab and anechoic chamber with the massive MIMO testbed.

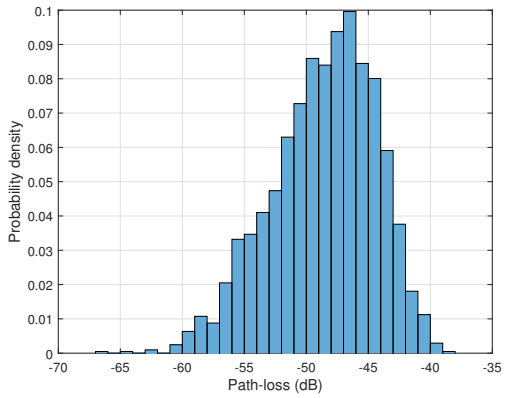

Fig. 6: Inter-cluster path-loss measured between the two 32-antenna arrays in the indoor experimental scenario by the massive MIMO testbed. To be comparable to the measured mutual coupling, the antenna gain is not excluded.

$\mathrm{card}(\varpi_i)$ were both set to 1 for TH and ICCM, respectively. Moreover, the transmitter power P_{TX} was configured to 0 dBm and a fixed receiver gain was configured to 30dB. From the measurement in Section IV-B, we know even for the weakest path, the SNR=$P_{TX} - 65 - (-95)$=30dB[6] should be sufficient for calibration. However, the power difference between the strongest and the weakest path is around $(65 - 25 = 40\text{dB})$, which means if the strongest path is not truncated by the receiver, then the SQNR of the weakest one degrades 40dB. Hence, the big dynamic range in the designed scenario enables us to compare which algorithm is more robust to the quantization error. In Fig. 7 and 8, we show that the EVM and throughput of the two MSs evolve over around 8 minutes. Apparently, the proposed ICCM outperforms the others in both MSs. ICCM recovers the SQNR by the array gain, assuming we receive equally from the inter-cluster paths, then the SQNR is boosted by $10log_{10}(32) = 15$dB. In this experiment, ICCM actually boosted more SQNR by diversity, as not all paths shared the same power from the measurement. Interestingly, the EVM degrades quite quick over time, and the accuracy of the reciprocity calibration determines the recalibration period. Particularly noteworthy, though the EVM of TH method degrades much faster than GLS, the throughput of GLS drops faster than that of TH. A possible explanation for this, as we only have two clusters, the accuracy of the reciprocity coefficients in the master cluster of the hierarchical based calibration methods is not dependent on the inter-cluster calibration; the larger path-loss between the two clusters only impacts the accuracy in the slave cluster. Hence, an accurate estimation only in the master cluster influences the performance significantly. Though the performance in throughput of TH and ICCM looks similar, the EVM of ICCM is better. As a result, the ICCM can support higher modulation schemes and is thus a superior candidate for DM-MIMO systems.

[6]The noise level can be referred to [14], eq. (22)

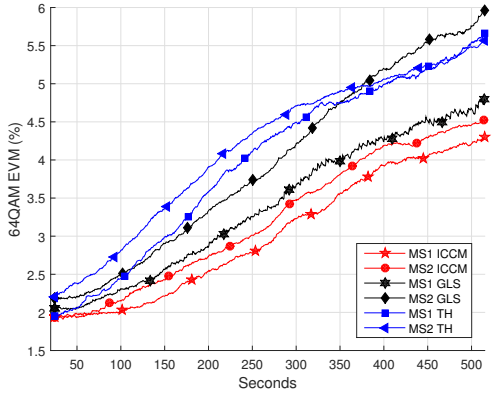

Fig. 7: EVM of uncoded 64-QAM after finishing the reciprocity calibration at the BS.

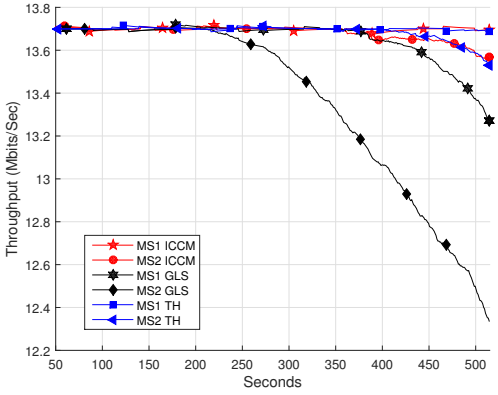

Fig. 8: Throughput comparison of the two MSs receive uncoded 64-QAM in DL. Peak data rate per MS is 13.68 Mbits/s as around $1/7$ of the LTE frame time is occupied for DL.

V. Conclusions

In this paper, we have proposed a potential reciprocity calibration algorithm called ICCM for DM-MIMO system. The big difference between intra-cluster mutual coupling and

inter-cluster path-loss was then validated in the KUL massive MIMO testbed in an indoor scenario. Our results show that ICCM outperforms the other two state-of-the-art methods from two different aspects. Compare to FA-GLS, the hierarchical based approach is more robust to a big dynamic range in channel gain within and in between the sub arrays. Moreover, compare to TH, ICCM exploits channel diversity to improve the accuracy of the inter-cluster calibration coefficients. Overall, hierarchical based ICCM is the best candidate for estimating the reciprocity calibration coefficients in DM-MIMO systems.

ACKNOWLEDGES

This work was partially funded by the a Flemish Hercules grant, and by the European Union's Horizon 2020 under grant agreement no. 732174 (ORCA project) Furthermore, the authors would like to thank Mr. Gino Van Houdt for his support of assembling the KUL massive MIMO testbed.

REFERENCES

[1] T. L. Marzetta, "Noncooperative cellular wireless with unlimited numbers of base station antennas," Wireless Communications, IEEE Transactions on, vol. 9, no. 11, pp. 3590–3600, November 2010.

[2] F. Rusek, D. Persson, B. K. Lau, E. G. Larsson, T. L. Marzetta, O. Edfors, and F. Tufvesson, "Scaling up MIMO: Opportunities and challenges with very large arrays," IEEE Signal Process. Mag., vol. 30, pp. 40–60, Jan. 2013.

[3] E. G. Larsson, F. Tufvesson, O. Edfors, and T. L. Marzetta, "Massive MIMO for next generation wireless systems," IEEE Commun. Mag., vol. 52, pp. 186–195, Feb. 2014.

[4] E. Björnson, M. Matthaiou, and M. Debbah, "Massive MIMO with nonideal arbitrary arrays: Hardware scaling laws and circuit-aware design," IEEE Trans. Wireless Commun., vol. 14, no. 8, pp. 4353–4368, Aug. 2015.

[5] S. Firouzabadi and A. Goldsmith, "Optimal placement of distributed antennas in cellular systems," in Proc. IEEE 12th Int. Workshop Signal Process. Adv. Wireless Commun. (SPAWC'11), Jun. 2011, pp. 461–465.

[6] D. Wang, J. Wang, X. You, Y. Wang, M. Chen, and X. Hou, "Spectral efficiency of distributed MIMO systems," IEEE J. Sel. Areas Commun., vol. 31, no. 10, pp. 2112–2127, Oct. 2013.

[7] G. N. Kamga, M. Xia, and S. Assa, "Spectral-efficiency analysis of massive MIMO systems in centralized and distributed schemes," IEEE Trans. Commun., vol. 64, no. 5, pp. 1930–1941, May 2016.

[8] C.-M. Chen, V. Volskiy, A. Chiumento, L. Van der Perre, G. Vandenbosch, and S. Pollin, "Exploration of user separation capabilities by distributed large antenna arrays," in Proc. Globecom Workshops, Dec. 2016.

[9] H. Xia, A. Herrera, S. Kim, and F. Rico, "A CDMA-distributed antenna system for in-building personal communications services," IEEE J. Sel. Areas Commun., vol. 14, no. 4, pp. 644–650, May 1996.

[10] R. Schuh and M. Sommer, "W-CDMA coverage and capacity analysis for active and passive distributed antenna systems," in Proc. IEEE Veh. Technol. Conf. (VTC'02-Spring), 2002, vol. 1, pp. 434–438.

[11] Björnson, E., Matthaiou, M., Pitarokoilis, A., and Larsson, E.G.: 'Distributed massive MIMO in cellular networks: impact of imperfect hardware and number of oscillators'. Proc. European Signal Processing Conf. (EUSIPCO), Nice, France, August 2015.

[12] R. Rogolin et al., "Scalable synchronization and reciprocity calibration for distributed multiuser MIMO," IEEE Trans. Wireless Commun., vol. 13, no. 4, pp. 1815–1831, Apr. 2014.

[13] R. Rogalin, O. Bursalioglu, H. Papadopoulos, G. Caire, and A. Molisch, "Hardware-impairment compensation for enabling distributed large-scale MIMO," in Proc. Inf. Theory Appl. Workshop (ITA), 2013, pp. 1–10.

[14] J. Vieira, F. Rusek, and F. Tufvesson, "Reciprocity calibration methods for Massive MIMO based on antenna coupling," in proc. IEEE Global Commun. Conf. (GLOBECOM'14), Dec. 2014, pp. 3708–3712.

[15] C. Shepard, H. Yu, N. Anand, E. Li, T. Marzetta, R. Yang, and L. Zhong, "Argos: practical many-antenna base stations," in Proceedings of the 18th Annual International Conference on Mobile Computing and Networking, Mobicom '12. New York, NY, USA: ACM, 2012, pp. 53–64.

[16] F. Kaltenberger, H. Jiang, M. Guillaud, and R. Knopp, "Relative channel reciprocity calibration in MIMO/TDD systems," in Proc. 2010 Future Netw. Mobile Summit, pp. 1–10.

[17] J. Vieira et al ., "A Flexible 100-Antenna Testbed for Massive MIMO," Proc. IEEE Globecom Wksp. — Massive MIMO: From Theory to Practice , 2014.